ELSEVIER

Chemical Geology 212 (2004) 45–57

CHEMICAL GEOLOGY
INCLUDING
ISOTOPE GEOSCIENCE

www.elsevier.com/locate/chemgeo

Extreme lithium isotopic fractionation during continental weathering revealed in saprolites from South Carolina

Roberta L. Rudnick[a,*], Paul B. Tomascak[a,1], Heather B. Njo[a], L. Robert Gardner[b]

[a]*Geochemistry Laboratory, Department of Geology, University of Maryland, College Park, MD 20742, USA*
[b]*Department of Geology, University of South Carolina, Columbia, SC 29208, USA*

Received 2 March 2004; received in revised form 6 July 2004

Abstract

The lithium concentration and isotopic composition of two saprolites developed on a granite and diabase dike from South Carolina have been measured in order to document the behavior of lithium isotopes during continental weathering. Both saprolites show a general trend of decreasing δ^7Li with increasing weathering intensity, as measured by both bulk density and the chemical index of alteration (CIA). The saprolite developed on the granite is isotopically lighter than the fresh igneous rock (δ^7Li=−6.8‰ to +1.4‰ vs. +2.3‰, respectively), and is generally depleted in lithium. These observations are consistent with leaching of lithium via Rayleigh distillation during progressive weathering; most saprolites fall on a Rayleigh distillation curve corresponding to an apparent fractionation factor (α) of 0.997. However, two samples have higher lithium contents than the fresh granite and thus point to additional processes affecting lithium in the saprolite (e.g., sorption of lithium on to clay minerals). The saprolite profile developed on the diabase dike shows highly variable δ^7Li values, ranging down to extremely light compositions (−20‰). Previous work has identified a chemical and mineralogical discontinuity at a depth of 2 m, but our lithium data show a marked discontinuity at 6 m depth. Saprolite samples at or above 6 m depth are highly weathered (CIA=88–95), depleted in lithium (having <50% of the original diabase lithium) and isotopically light (−10‰ to −20‰ vs. −4.3‰ for the unweathered diabase). Most of the data are consistent with leaching of lithium via Rayleigh distillation during intense weathering, with apparent α values of 0.995 to 0.980. Samples experiencing lower apparent α values tend to have higher kaolinite/smectite ratios, suggesting a mineralogical control on isotopic fractionation. However, the lightest sample (at −20‰) is only slightly depleted in lithium and would require extremely low α values to explain via Rayleigh distilliation. This extreme composition remains enigmatic. Saprolite samples below 6 m have highly variable δ^7Li (−5‰ to −14‰) and, importantly, lithium concentrations that are higher than that of the unweathered diabase (up to 2.4 times the concentration of the fresh diabase). These deeper saprolites thus cannot be explained by Rayleigh distillation. A positive correlation between δ^7Li and Li

* Corresponding author. Tel.: +1 301 405 1311; fax: +1 301 405 3597.
E-mail address: rudnick@geol.umd.edu (R.L. Rudnick).
[1] Department of Earth Science, SUNY Oswego, NY 13126-3599, USA.

doi:10.1016/j.chemgeo.2004.08.008

concentration suggests these samples formed by mixing between an isotopically light saprolite and heavy, groundwater lithium, and we thus suggest that the 6-m discontinuity may mark the position of a paleo water table.

Keywords: Lithium isotopes; Continental weathering; Saprolite; South Carolina

1. Introduction

Lithium is a fluid-mobile, moderately incompatible trace element having two isotopes with ~15% relative mass difference. Like other alkali metals, lithium is present on the Earth only in the +1 valence state, so its isotopic composition is not influenced by redox reactions. Moreover, lithium is not a nutrient and does not participate in biologically mediated reactions. These characteristics make lithium isotopes potentially excellent tracers of near-surface fluid–rock reactions.

A number of studies, starting with the pioneering work of L.H. Chan et al. in the late 1980s, have established that large fractionations of lithium isotopes occur within the rock–hydrosphere system. Seawater has a homogenous lithium isotopic composition, consistent with the relatively long residence time of lithium in the oceans (Li, 1982), and is isotopically quite heavy (δ^7Li=+31‰; Chan and Edmond, 1988; You et al., 1996). The upper mantle is inferred to have a significantly lighter δ^7Li, equal to that of average MORB, ~+4±2‰ (Chan et al., 1992, 2002; Tomascak and Langmuir, 1999), because lithium isotopes do not fractionate significantly at the high temperatures of mantle melting, >1000 °C (Tomascak et al., 1999b). Compared to the mantle, the upper continental crust has an even lighter δ^7Li of 0±2‰ (Teng et al., 2004), as sampled by dissolved and suspended river loads (Huh et al., 2001), shales, loess and granites (Teng et al., 2004). This isotopically light composition of the upper continental crust is inferred to reflect the influence of weathering, with heavy lithium partitioned into surface waters, leaving lighter lithium behind in the weathered products (Teng et al., 2004). This inference is supported by the isotopically heavy compositions of groundwaters (Hogan and Blum, 2003; Tomascak et al., 2003), by the observed isotopic fractionation between dissolved and suspended loads of rivers (Huh et al., 2001) and experimental partitioning data for lithium sorption on to gibbsite and ferrihydrite (Pistiner and Henderson, 2003). However, Pistiner and Henderson (2003) found no fractionation during lithium sorption onto smectite.

To date, the limited lithium isotopic data available for weathering profiles shows somewhat conflicting evidence. Pistiner and Henderson (2003) found a very slight decrease (~2‰) in δ^7Li on a weathered surface of a 200-year-old Icelandic basalt, but no detectable change in δ^7Li for soil developed on a Hawaiian basalt (although they inferred that production of isotopically light lithium was countered by the isotopically heavy rainwater in Hawaii). In contrast, Huh et al. (2002) found soils developed on a Hawaiian basalt to have variable but heavy lithium (up to +10‰), which they attributed to uptake of aerosol lithium derived from seawater.

Here, we present lithium isotopic data for two saprolite profiles developed on Paleozoic igneous rocks weathered in a temperate climate on the eastern seaboard of the United States. Saprolites are clay-rich regoliths that formed in situ on crystalline bedrock during tropical to subtropical weathering (White, 2003), preserving the textures of the original rock type on which they develop. Saprolites are thus interpreted to represent isovolumetric weathering for which chemical analyses can be used to assess the chemical changes produced by weathering (e.g., Gardner et al., 1978; White et al., 2001). Our results demonstrate that lithium isotopic fractionation correlates directly with the degree of weathering, and that extremely light δ^7Li values, down to δ^7Li=−20‰, can be produced in these environments.

2. Samples

The saprolites we studied developed on Paleozoic igneous rocks from two localities in South Carolina. Both lie within the Paleozoic Piedmont province, near its boundary with the Atlantic coastal plain (Fig. 1). Mean annual rainfall (~120 cm year^{-1}) and temper-

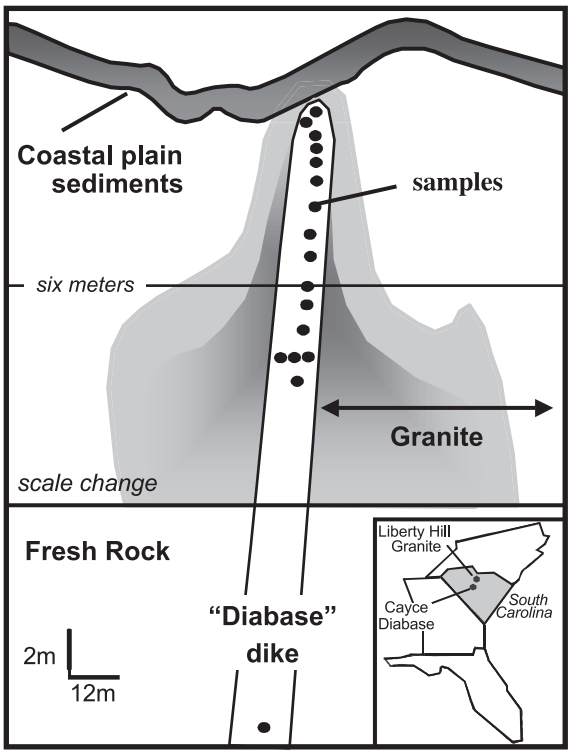

Fig. 1. Sketch of cross-section through granite quarry wall near Cayce, SC, showing diabase dike mantled by alteration halo in surrounding granite saprolite. Alternation halo in granite broadens at a depth of ~6 m; dark gray depicts region of green-stained granite whereas lighter gray represents region of red-stained granite. Line at 6 m marks position of discontinuity in lithium isotopes (Fig. 2), thicker horizontal line marks a change in vertical scale. The fresh diabase lies at a depth of 30 m. Black dots are samples measured here (from Gardner et al., 1981). Inset shows sample locality for diabase and Liberty Hill granite outcrop.

atures (18 °C) reflect a currently temperate climate (data from the South Carolina office of climatology www.dnr.state.sc.us/climate/sco/).

2.1. Cayce diabase

The first locality, from which most of our measurements derive, is a granite quarry near Cayce, SC (N33°58.09′ , W81°03.07′). Here, a cross-section through approximately 10 m of saprolite, developed on granite and the subvertical diabase dike that cuts it, is exposed in the walls of the quarry (Fig. 1; Gardner et al., 1981). The saprolite is overlain by Tertiary coastal plain sediment of uncertain age. Despite the fact that the saprolite occurs beneath the coastal plain sediment, it is unclear exactly when the saprolites developed. For example, on the basis of saprolite geometry and soil development, Pavich and Obermeier (1985) argued that saprolite buried beneath coastal plain sediment in the Piedmont of Virginia actually developed after burial in the Miocene.

The diabase dike is approximately 7 m wide and contains significant amounts of talc (20%) and chlorite (8%) in addition to plagioclase (40%), clinopyroxene (29%) and opaque minerals (2%), reflecting a greenschist-facies metamorphic overprint of the original igneous rock. Green- and red-stained alteration haloes occur sequentially within the granite surrounding the dike. These form a rather narrow (3–6 m thick) aureole in the upper 6 m of the profile, but spread up to ~30 m thickness below 6 m depth (Fig. 1).

Gardner et al. (1981) report the density, clay mineral proportions and bulk composition of the unweathered diabase as well as samples taken along an 11-m profile through the saprolite. They found a discontinuity in composition and clay mineralogy of the weathering profile at a depth of about 2 m. Below the discontinuity, the kaolinite to smectite ratio increases as density increases (toward the unweathered diabase). Above the discontinuity, the kaolinite/smectite ratio decreases as density decreases. The presence of siderite in boxwork veins below the discontinuity suggests the presence of more reducing conditions. Above this depth, Al and H_2O^+ are depleted, and Fe^{3+} is enriched. They interpreted the discontinuity to reflect a change in redox, with oxidized conditions in the upper profile reflected by the formation of Fe-rich smectite over kaolinite and reducing conditions in the lower portion of the profile reflected in the formation of kaolinite over Al-rich smectite.

2.2. Liberty Hill granite

The second saprolite we studied is exposed in a borrow pit at an elevation of 105 m on the Liberty Hill granite (34.24°N, 80.43°W), in Kershaw County, about 18 km northwest of Camden, SC. The saprolite exposed here is at least 30 m in total thickness and developed on granite consisting of quartz, plagioclase, biotite and amphibole with large (0.5–10 cm) micro-

cline phenocrysts. The slope on which the pit is dug leads to a summit (135 m ASL), about 0.8 km northeast of the pit, on which an isolated remnant of coastal plain sediment was found atop deeply weathered granite saprolite. Thus, it is possible that the saprolite exposed in the pit was also capped by coastal plain sediment before dissection by stream erosion. In the borrow pit, Gardner and Nelson (1991) describe the development of "ghost" core stones—subspherical blocks of unweathered granite—in this saprolite, which they infer formed below the water table under reducing conditions. Some of these core stones extend above the hill slope, indicating recent erosion. Moreover, thin A and B soil horizons are developed on the hill slope, indicating a second stage of weathering, after the saprolite developed and was exposed by erosion.

The samples measured here come from the same borrow pit used by Gardner and Nelson (1991) in their study of the ghost core stones. Because of the steepness of the vertical wall and the presence of core stones, it was not possible to sample a cross-section through this saprolite. Nevertheless, in general, bulk density increases with depth in the saprolite, indicating more intense weathering and leaching near the surface. Sample LHP-B03 was taken from just below the B soil horizon on the hill slope, where the granitic texture is first observed. All other samples come from greater distance from the hill slope, well within the saprolite. X-ray diffraction data indicate that these saprolites are dominated by kaolinite, with minor vermiculite (forming on biotite) and gibbsite.

3. Analytical methods

The rock powders investigated here are the same as those used in previous investigations of these saprolites (Gardner et al., 1981; Gardner and Nelson, 1991). Approximately 25 mg of rock powder was dissolved in Savillex screw-top beakers in a mixture of 0.5 ml of concentrated HNO_3 and 2.0 ml concentrated HF. The capped beakers were heated for ~24 h at 90 °C on a hot plate in a laminar flow hood. The solutions were then dried, refluxed twice in concentrated HNO_3, then dried again. The residue was then dissolved in concentrated HCl, which was fumed off at ~90 °C until the solutions were perfectly clear, thus achieving 100% dissolution. The clear solutions were then evaporated to dryness and the dried residue was dissolved in 1.0 ml of 4 M HCl. The 4-M solution was centrifuged and inspected closely in a clear centrifuge tube to assure no insoluble residue remained in the solution prior to column chromatography.

Separation of lithium was achieved using the first three columns of the chemical separation procedure described by Moriguti and Nakamura (1998). Each column is loaded with 1 ml of Bio-Rad AG 50w-x12 (200–400 mesh) resin. Prior to use, the resin beds are cleaned by flushing the columns with 10 ml of 6 M HCl followed by 10 ml Milli-Q® water (18 M Ω resistivity). The position of the lithium cut for each column was determined using both pure lithium standard solutions and dissolved rocks with a wide range of compositions (loess, basalt, peridotite) in order to assure 100% yield. The excellent comparison of our standard data with published results (Table 1, caption) demonstrates that we achieved 100% yield.

Prior to analysis, the Na/Li voltage ratio of each solution was measured semiquantitatively, as ratios greater than ~5 cause unstable instrumental fractionation, thus inhibiting accurate Li isotope determinations (Tomascak et al., 1999a). In nearly all samples, the Na/Li ratios were suitable for analysis at the end of the three-step column separation. In a few instances, high Na/Li was observed, necessitating further purification through the third column.

Purified Li solutions [~100 ppb Li in 2% (v/v) HNO_3 solutions] were introduced to the Ar plasma using an auto-sampler (ASX-100® Cetac Technologies) through a desolvating nebulizer (Aridus® Cetac Technologies) fitted with a PFA spray chamber and micronebulizer (Elemental Scientific). Samples were analyzed on a Nu Plasma multicollector Inductively Coupled Plasma Mass Spectrometry (MC-ICPMS). Details of the mass spectrometry are found in Teng et al. (2004) and only a brief synopsis is provided here. Following Tomascak et al. (1999a), each sample analysis is bracketed before and after by measurement of the L-SVEC standard (Flesch et al., 1973) having similar solution concentration (within ~50%) and the δ^7Li of the sample is calculated relative to the average of these two bracketing L-SVEC runs. At least two other Li standards [e.g., the in-house Li-UMD-1 (a

Table 1
Major element composition (wt.%), bulk density (g cm^{-3}), Li concentration (ppm) and isotopic composition (‰) for saprolites from South Carolina

Sample #	Type	Depth (m)	Density	K/S[a]	SiO_2	TiO_2	Al_2O_3	Fe_2O_3	FeO[b]	MnO	MgO	CaO	Na_2O	K_2O	P_2O_5	H_2O+	Total	CIA	Li	Li (norm)[c]	δ^7Li	*n*
Caycee diabase profile through saprolite																						
M1	Saprolite	0.10	0.96	0.04	54.63	0.66	15.78	20.23			1.82	0.98		0.36	0.02	4.69	99.17	88	5.1	0.24	−11.6	
M3	Saprolite	0.50	0.80	0.03	58.57	0.88	19.25	10.88	0.06		2.22	1.02	0.03	0.71	0.06	4.43	98.11	88	7.1	0.27	−10.3	2
Replicate[d]	Saprolite																				−9.9	2
M4	Saprolite	1.00	0.80	0.00	60.76	0.52	19.45	12.39	0.09		1.61	0.78		0.58	0.14	4.53	100.85	92	8.2	0.31	−13.3	
M5	Saprolite	1.50	1.01	0.03	58.86	0.64	17.85	12.23	0.08		1.98	1.14		0.33	0.16	5.17	98.44	90	5.6	0.23	−14.4	
M6	Saprolite	2.00	1.00	0.07	59.30	0.58	17.52	11.51	0.08		2.01	1.01		1.16	0.16	4.88	98.21	87	9.6	0.41	−12.5	2
Replicate[d]																					−11.7	2
M7	Saprolite	3.00	1.03	5.00	53.95	0.77	27.79	5.46	0.14		0.58	0.80		0.34	0.15	8.28	98.26	95	20	0.53	−13.8	
M8	Saprolite	4.00	1.00	2.10	54.22	0.78	28.16	6.66	0.16		0.88	0.80		0.36	0.12	7.21	99.35	95	18	0.48	−17.1	
M9	Saprolite	5.00	1.17	2.50	55.82	0.81	23.75	6.87	0.10		0.97	0.83		0.46	0.10	6.92	96.63	93	14	0.44	−17.3	
M10	Saprolite	6.00	1.38	1.70	54.93	0.76	25.16	7.90	2.46		1.00	1.24		0.48	0.11	7.92	101.96	91	24	0.71	−20.2	2
M11	Saprolite	7.00	2.11	0.30	48.31	0.55	17.16	7.24	4.15		11.94	7.05	1.09	0.37	0.19	3.65	101.70	54	47	2.04	−6.7	2
M12	Saprolite	8.00	2.26	0.15	49.38	0.56	18.23	8.81	3.80		8.60	7.16	1.33	0.43	0.20	3.29	101.79	55	23	0.94	−10.4	
M13	Saprolite	9.00	1.81	0.40	52.72	0.72	22.24	9.13	2.21		5.51	3.97	0.97	0.42	0.15	4.94	102.98	71	42	1.39	−11.8	
M14	Saprolite	10.00	1.66	1.10	54.53	0.85	22.81	10.24	1.24		2.69	1.16	0.02	0.56	0.11	6.80	101.01	90	42	1.36	−9.7	
L14-8	Saprolite	10.00	2.46	0.25	48.56	0.57	17.32	7.76	3.39		10.96	8.92	1.27	0.37	0.18	3.08	102.38	49	56	2.41	−9.1	2
L14-9	Saprolite	10.00	2.52	0.00	49.11	0.58	16.85	7.09	3.98		10.47	9.53	1.36	0.39	0.21	2.33	101.90	46	32	1.39	−8.6	
Replicate[d]																					−7.6	
M15	Saprolite	11.00	1.85	1.00	51.78	0.73	21.94	10.80	2.18		5.84	1.42	0.02	0.56	0.09	6.48	101.84	88	24	0.83	−13.7	
M20	Diabase	30.00	3.01	0.00	48.68	0.48	17.09	7.09	6.26		11.84	10.43	1.40	0.32	0.25	2.06	105.90	45	23	1.00	−4.7	2
Replicate[d]																					−4.0	2
Liberty Hill granite saprolites																						
LHP-B-3	Saprolite	Extreme saprolite	1.10		69.33	0.45	17.65	2.95	0.11	0.012	0.29	0.01	0.28	5.74	0.0308	4.47	96.85	73	5.0	0.29	−6.8	
4	Saprolite		1.55		67.60	0.54	19.26	2.71	0.18	0.014	0.34	0.01	0.40	6.58	0.0171	4.69	97.65	71	7.3	0.39	−0.8	
5	Saprolite		1.41		71.72	0.47	17.16	2.45	0.14	0.018	0.32	0.06	0.87	5.89	0	3.73	99.10	68	12	0.70	−0.5	
6	Saprolite		1.47		71.20	0.38	15.58	2.05	0.17	0.028	0.34	0.16	1.21	6.02	0.012	3.16	97.09	64	11	0.71	+1.4	
9	Saprolite		1.60		71.25	0.37	15.48	1.91	0.12	0.029	0.38	0.18	1.24	6.13	0.0336	2.66	97.12	63	8.8	0.59	+0.5	
10	Saprolite		1.66		71.96	0.39	14.71	2.29	0.08	0.047	0.38	0.46	2.59	5.38	0.035	1.75	98.32	58	11	0.79	+0.2	
13	Saprolite	Middle horizon	1.89		72.65	0.34	14.69	2.09	0.14	0.030	0.30	0.41	1.77	5.40	0.0157	1.69	97.84	61	6.3	0.44	+0.2	2
14	Saprolite		2.47		72.21	0.40	14.07	1.94	0.22	0.044	0.39	0.69	2.69	5.40	0.0448	0.89	98.10	55	14	1.01	+0.1	2
19	Saprolite		2.64		69.68	0.41	14.63	2.09	0.50	0.047	0.50	1.72	3.39	4.88	0.110	0.30	97.96	52	21	1.49	+1.4	3
20	Granite	"Fresh"	2.71		66.95	0.55	15.34	2.79	0.54	0.063	0.70	1.96	3.46	5.27	0.158	0.19	97.78	51	15	1.00	+2.3	2

Major element data and bulk denisties for Cayce diabase are from Gardner et al. (1981). Major elements are in wt.%, lithium concentration is in ppm.
δ^7Li values for international rock standards measured during the course of this study are as follows: BCR-1: +2.7‰ (*n*=3), BHVO-1: +4.3‰ (*n*=1), BIR-1: +3.9‰ (*n*=4), JB-2: +4.0‰ (*n*=1).
n=Number of determinations for which average value is reported. All repeat measurements fall within ±1‰ of each other.

[a] Kaolite/smectite intensity ratio from XRD (see Gardner et al., 1981).

[b] FeO concentration determined by titration.

[c] Normalized lithium concentration=(Li/Al of the saprolite)/(Li/Al protolith).

[d] "Replicate" refers to repeat dissolution and measurement of a sample powder.

purified Li solution from Alfa Aesar®) and IRMM-016; Qi et al., 1997] were routinely analyzed during the course of an analytical session. The in-run precision on $^{7}Li/^{6}Li$ measurements is $\leq\pm 0.2‰$ for two blocks of 20 ratios each, with no systematic change in $^{7}Li/^{6}Li$ ratio. The external precision, based on 2σ of repeat runs of pure Li standard solutions, is $\leq\pm 1.0‰$. For example, IRMM-016 gives $\delta^{7}Li=-0.1\pm 0.2‰$ (2σ, $n>50$ runs over a 2-year period); and in-house standard Li-UMD-1 gives $\delta^{7}Li=54.7\pm 1‰$ (2σ, $n>100$ runs over a 2-year period). Data for international rock standards, measured during the course of this study, are presented in the footnote to Table 1. Our values are within uncertainty of previously published results for BHVO-1 (+4.3‰ vs. +5.0–+5.8‰, James and Palmer, Chen and Frey, Bouman et al., 2004) and JB-2 (+4.0‰ vs. +3.9–+5.2‰—see compilation in Seitz et al., (2004)); to our knowledge, ours are the first published data for BCR-1 (+2.7‰) and BIR-1 (+3.9‰).

4. Results

4.1. Presentation of data

Lithium concentrations and isotopic compositions of the two saprolites and fresh protoliths are presented in Table 1, along with major element data, bulk densities and the chemical index of alteration (CIA). Also given is the kaolinite to saprolite XRD peak intensity ratio for the diabase saprolites.

CIA is the molar $Al_2O_3/(Al_2O_3+CaO^*+Na_2O+K_2O)$, where CaO* refers to Ca that is not contained in carbonate and phosphate (Nesbitt and Young, 1982; McLennan, 1993). Correction for Ca in apatite is done on the basis of the P_2O_5 concentration. Correction for Ca in carbonate is generally done on the basis of CO_2 concentrations. In the absence of such data (such as CO_2 for the saprolites investigated here), McLennan (1993) has suggested correcting for Ca-carbonate by assuming the molar CaO/Na_2O ratio is less than 1. While this works well for the study of the upper crust, which is granitic in composition and has low CaO/Na_2O, such an assumption is not justified for the study of weathering in a diabase, which can have originally high CaO/Na_2O. Moreover, the only carbonate observed in these samples is siderite (Gardner et al., 1981). We therefore do not attempt to correct for Ca in carbonate in the diabase saprolites. The saprolites developed on granite all have Ca/Na<1, suggesting little carbonate is present and thus no correction is needed in calculating the granite CIA values.

CIA has proven useful in evaluating the degree of weathering experienced by igneous rocks. Weathering of silicates, in particular, feldspar, is accompanied by leaching of the more soluble elements (e.g., Na, K and Ca) and retention of elements that reside in clay minerals (e.g., Al). The CIA of unweathered igneous rocks is generally low (<50) and it increases with the degree of weathering (Nesbitt and Young, 1982); shales have CIA between 60 and 80 (Teng et al., 2004).

When evaluating chemical changes associated with weathering, a number of workers normalize absolute concentrations of "mobile" elements, such as lithium, to that of a presumed immobile element (e.g., Al, Ti, Zr and Nb), in order to evaluate the relative depletion or enrichment of the mobile element. For this approach to be valid, one has to first ascertain that "immobile" elements really are so. Gardner et al. (1981) show that the volumetric concentration (g cm^{-3}) of Al decreases by a factor of two or more in the most highly weathered diabase samples (see Fig. 2 of Gardner, 1981), which have extremely low bulk densities (down to 0.8 g cm^{-3}). This observation, coupled with the assumption that saprolite formation is isovolumetric (due to the preservation of original igneous textures), led them to suggest that Al was depleted by up to a factor of two during development of the saprolite. Nevertheless, Al is a major constituent of the clay minerals that form the main secondary phases in the saprolite. We have thus chosen to normalize lithium contents to aluminum and use these, in preference to absolute concentrations, to evaluate the *relative* mobility of lithium. The normalized concentrations presented in Table 1 represent the Li/Al ratio of the saprolite divided by the Li/Al ratio of the fresh protolith and thus provide a ready gauge of lithium mobility relative to aluminum; a value of 2 indicates a twofold increase in lithium concentration, whereas a value of 0.5 indicates 50% depletion of the original lithium. In practice, the normalized concentrations show the same patterns as the absolute

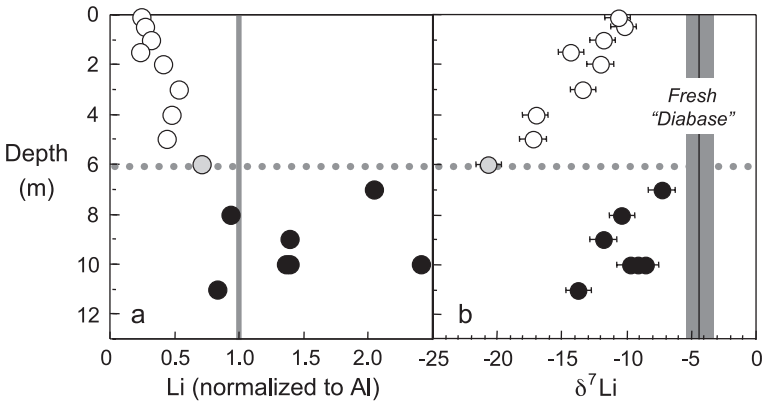

Fig. 2. (a) Lithium concentration, normalized to aluminum (see text for nomalization procedure), and (b) δ^7Li as a function of depth in the diabase weathering profile. Vertical gray bar on both panels represents composition of unweathered "diabase", which was sampled at a depth of 30 m from the surface. The term diabase is given in quotes, as the presence of significant quantities of talc and chlorite suggest this rock may be better labeled as a "greenstone" or "meta-diabase". Gray dotted line depicts the discontinuity at 6 m depth, which may represent a paleo water table. In this and subsequent plots, open circles represent samples taken above this discontinuity, closed circles are samples from below the discontinuity and the single gray circle represents the sample at the 6-m discontinuity. Error bars represent 2σ uncertainty on δ^7Li measurements.

concentrations (indicating both enrichment and depletion of lithium in the saprolites developed on both the diabase and granite), but tend to follow more well-defined trends.

4.2. Cayce diabase saprolite

In the saprolite developed on diabase at the Cayce quarry, lithium concentrations increase with depth (Fig. 2a, Table 1), with very low concentrations near the surface (5–7 ppm, indicating up to 75% depletion of original lithium relative to Al), increasing to variable, but high concentrations deep within the profile (up to 56 ppm, indicating over a twofold enrichment in lithium relative to the diabase). The unweathered diabase has a concentration falling between these two extremes (23 ppm).

Unlike the lithium concentration, the isotopic composition of lithium does not vary consistently with depth, but rather shows a step function (Fig. 2b).

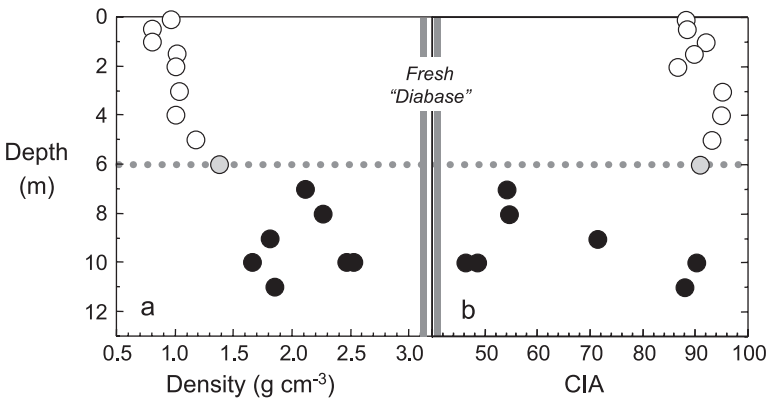

Fig. 3. (a) Bulk density and (b) chemical index of alteration (CIA) as a function of depth in the diabase weathering profile. Vertical gray bar represents composition of unweathered "diabase", which was sampled at a depth of 30 m from the surface. Gray dotted line depicts the discontinuity δ^7Li, which may represent a paleo water table. Symbols as in Fig. 2.

Saprolite at the surface is isotopically light (−12‰) and δ^7Li decreases monotonically to a depth of 6 m, where the lowest δ^7Li value is found (−20‰). Just below this depth, δ^7Li jumps to the heaviest value measured in the saprolite (−7‰), then decreases again to a value of −14‰ at the base of the measured profile (Fig. 2b). The δ^7Li value of the unweathered diabase (at 30 m depth) is heavier than that of any of the overlying saprolite at −4.3‰.

Both bulk density and CIA can be used to evaluate the degree of weathering experienced by the saprolite. Bulk density is extremely low (down to 0.8 g cm^{-3}) in the uppermost section of the profile and increases slightly to a depth of 6 m, below which the density is higher and shows no systematic trend as a function of depth (Fig. 3a). CIA shows an overall decrease with depth, but changes less systematically than bulk density (Fig. 3b). CIA is greatest in the upper portion of the profile (i.e., 85–95 above 6 m), but does not change systematically over this depth interval. Below 6 m, where the jump in δ^7Li occurs, CIA varies dramatically from a low of 49 to a high of 90, again showing no correlation with depth. The unweathered diabase has a CIA of 45, which is typical of basalts (30 to 45, Nesbitt and Young, 1982). CIA shows a negative, nonlinear correlation with δ^7Li (Fig. 4a), with the most weathered saprolite (CIA=88 to 95, open circles) in the upper portion of the section showing a range in δ^7Li from −10‰ to −20‰ and the least weathered saprolite in the deeper part of the section (solid circles) ranging to heavier Li (δ^7Li=−7‰ to −10‰). Bulk density shows a positive correlation with δ^7Li (not shown), with the most weathered samples (density below 1.5 g cm^{-3}) showing a 10‰ range in δ^7Li.

4.3. Liberty Hill granite saprolite

Except for two samples, saprolites developed on the Liberty Hill granite have lithium concentrations that are lower than those of the fresh granite (i.e., 5–14 vs. 15 ppm, respectively), indicating loss of up to 70% of the original lithium in the granite; one sample has similar Li content as the granite and another has distinctly higher Li, at 21 ppm. These saprolites show a narrower range of CIA values (52–73) and bulk densities (1.1 to 2.7 g cm^{-3}) than those formed on the diabase and a correspondingly narrower range of δ^7Li (−7‰ to +1‰), with all but one sample having δ^7Li between −1‰ and +1‰. The δ^7Li of the saprolites is largely independent of CIA and bulk density, except that the sample with the highest CIA and lowest density has a very low δ^7Li value (sample LHP-B-3, Fig. 4b). This is the sample that is adjacent to the B soil horizon developed on the hill slope. The fresh granite has the highest δ^7Li (+2.3‰) and the lowest CIA (51). Collectively, the saprolite–granite data show an overall negative trend when plotted against CIA (Fig. 4b) and positive correlation with bulk density (not shown). Most saprolite samples have δ^7Li values within analytical uncertainty of one another, and are slightly lower (~2‰) than that of the fresh granite. Both the δ^7Li values and lithium concentration of the granite overlap those measured for other fresh granites (Bryant et al., 2003; Teng et al., 2004).

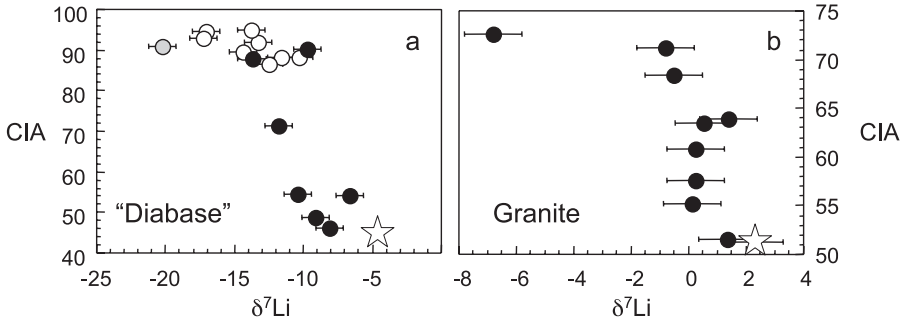

Fig. 4. δ^7Li vs. chemical index of alteration (CIA) for saprolites developed on (a) the Cayce diabase and (b) the Liberty Hill granite. Stars show compositions of unweathered protoliths to the saprolites. Error bars represent 2σ uncertainty. In panel (a), open circles represent samples taken above 6 m, filled circles are samples taken below 6 m and gray circle is sample at the 6-m discontinuity. See text for explanation of CIA.

5. Discussion

Whereas the Li concentration and δ^7Li of the Liberty Hill granite is typical of that observed in other unweathered granites, the same is not true for the diabase. Lithium in the unweathered Cayce diabase is distinctly more abundant (23 ppm) and isotopically lighter (δ^7Li=−4.3‰) than lithium in fresh mantle-derived mafic igneous rocks from the oceanic environment (e.g., <10 ppm, 4±2‰, respectively, Chan et al., 1992, 2002; Tomascak et al., 1999b; Chan and Frey, 2003; Pistiner and Henderson, 2003). Only a few data exist for unaltered continental mafic igneous rocks and these generally show Li contents and δ^7Li values similar to their oceanic counterparts (Ryan and Kyle, 2000; Bottomley et al., 2003), although a gabbro from the Canadian shield has somewhat higher concentration (17 ppm) and heavier δ^7Li (+10‰; Bottomley et al., 2003). A fresh metabasalt and an amphibolite are reported to have higher Li content (15–20 ppm) but similar δ^7Li (+5‰) to unmetamorphosed mafic igneous rocks (Bottomley et al., 1999, 2003). In contrast, altered fault zone metabasalts from the Miramar Con mine, Yellowknife, Canada, have even higher Li concentrations (35–62 ppm) and heavier isotopic compositions (+15‰; Bottomley et al., 2003). Thus, while the higher lithium concentration of the diabase overlaps those seen in some metamorphosed continental mafic igneous rocks, the very light isotopic composition does not. The reason for this unusually light isotopic composition is not known, but may reflect of incipient weathering, loss of heavy lithium during metamorphic devolatilization or assimilation of isotopically light metamorphic rocks prior to the dike's intrusion. No matter which is correct, we can use this sample as representative of the protolith on which the saprolite formed.

A number of previous studies have shown that heavy lithium preferentially partitions into the oceans during fluid–rock exchange, thus explaining the very heavy isotopic composition of seawater (e.g., Chan et al., 1992). More recent studies, focused on the continental environment, show similar results. For example, dissolved loads in rivers are 7‰ to 34‰ heavier than suspended loads (Huh et al., 2001). Moreover, Pistiner and Henderson (2003) found that Li-doped water in contact with gibbsite and ferrihydrite becomes isotopically heavier by 1‰ to 13‰, respectively, due to sorption of light lithium onto the minerals. They further demonstrated that lithium uptake in their experiments was most consistent with equilibrium exchange between water and mineral, rather than a Rayleigh distillation process.

The general expectation that continental weathering fractionates lithium isotopes, with heavier lithium leached to water, is supported by the data presented here. The negative correlations between CIA and δ^7Li (Fig. 4) and positive correlations between bulk density and δ^7Li for saprolites developed on both granite and diabase show that, in general, as weathering progresses, CIA increases, bulk density decreases and the saprolites become isotopically lighter. However, these correlations are not linear, and show some interesting structure that may reflect process. For example, at very high CIA values (>88) and low bulk densities in the saprolite developed on diabase, δ^7Li varies considerably and appears to be independent of CIA or density, hence, weathering. Likewise, CIA and bulk density vary considerably in the saprolite developed on granite, with little change in δ^7Li; only the sample with the highest CIA and lowest bulk density shows significantly lighter δ^7Li. Moreover, lithium concentration does not correlate well with δ^7Li, indicating that processes in addition to lithium leaching have

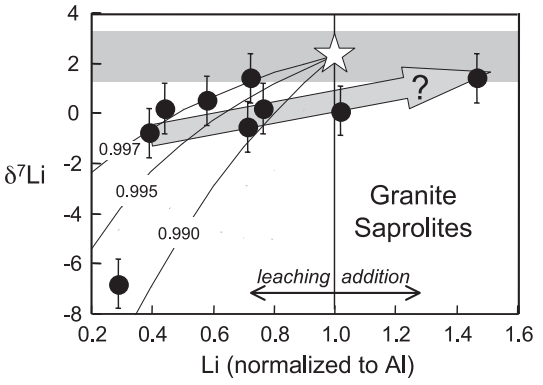

Fig. 5. Normalized lithium concentration vs. δ^7Li for saprolites developed on the Liberty Hill granite. Star shows composition of unweathered granite, other symbols as in Fig. 2. Error bars represent 2σ uncertainty. Curved lines depict lithium removal via Rayleigh distillation for different values (0.997 to 0.990) of the fractionation factor α [where $\alpha=(^7Li/^6Li)_{mineral}/(^7Li/^6Li)_{fluid}$]. Gray arrow shows possible reenrichment trend. See text for details.

occurred in these saprolites. We explore the possible meanings of these trends below.

5.1. Granite saprolite

As lithium is a fluid-mobile element, it is expected to be leached during weathering, just like Na, Ca and K (the main components in the CIA calculations). The relatively constant δ^7Li in the granite saprolite over a wide range of lithium contents (Fig. 5), bulk density and CIA values (Fig. 4b) suggests that lithium leaching (and in the case of the high Li sample, lithium adsorption) occurred in the absence of large isotopic fractionation. Such a result may reflect disequilibrium leaching (i.e., lithium was removed without equilibration between water and weathered product), or, perhaps more likely, that the secondary minerals did not significantly fractionate lithium (e.g., smectite in the sorption experiments of Pistiner and Henderson (2003)). Only one sample from the granite saprolite has significantly lower δ^7Li than the granite—the most highly weathered saprolite LHP-B-3. This sample, with the lowest lithium content, lowest bulk density and highest CIA occurs adjacent to the B soil horizon on the modern hill slope and may have experienced a second episode of weathering associated with the recent development of this soil horizon.

Rayleigh distillation curves for lithium removal from the granite, assuming fractionation factors, α [where $\alpha=(^7Li/^6Li)_{mineral}/(^7Li/^6Li)_{fluid}$], between 0.997 and 0.990, are shown in Fig. 5. These values of α overlap those determined experimentally for room-temperature Li sorption on to secondary minerals (0.986 to 1.000, Pistiner and Henderson, 2003) but are somewhat higher than the α value inferred for seafloor weathering at ~0 °C (0.980, Chan et al., 1992). Four of the nine saprolites fall near a Rayleigh distillation curve corresponding to an α value of 0.997 (Fig. 5), three others fall closer to a curve corresponding to α=0.992, whereas the final two have lithium contents that are higher than the granite and therefore cannot be explained by leaching of lithium.

The range in apparent α values may be explained in several ways. First, it is possible that α varies from sample to sample, depending on the secondary mineral assemblage. In a recent experimental study, Pistiner and Henderson (2003) demonstrated that different minerals have highly variable fractionation factors associated with lithium sorption (i.e., α=1 for smectite vs. α=0.986 for gibbsite). In another experimental study, Williams and Hervig (2003) found that lithium partitioning behavior in clays may depend on the crystallographic site on which lithium substitution occurs—interlayer or octahedral. The saprolites developed on granite are dominated by kaolinite and contain minor vermiculite and gibbsite. To date, there are no experimental data for lithium isotopic fractionation associated with kaolinite–water partitioning or adsorption, so we cannot evaluate whether the α values we infer here are consistent with kaolinite–water fractionation. We also do not have exact modal proportions of the secondary minerals in our samples, so we cannot determine whether the apparent spread of α values is due to changing mineralogy.

A second alternative is that the spread of apparent α values is due to leaching, followed by variable amounts of reintroduction of lithium via sorption onto clays. Indeed, the two samples with higher lithium content than the granite require some form of enrichment process to have occurred. In this scenario, the array of data lying along the gray arrow in Fig. 5 may reflect reintroduction of slightly heavier hydrospheric lithium to a depleted regolith. The single sample with significantly light lithium isotopic composition (−7‰) may reflect a second episode of weathering associated with development of the B soil horizon on the adjacent modern hill slope, which occurred under different conditions. This is the only sample that is proximal to the hill slope.

5.2. Diabase saprolite

Like the granite saprolites, those formed on the diabase show complications, implying processes in addition to lithium leaching were operative during their formation. In discussing these data, we divide the profile into two sections that show coherent behavior: above and below the 6-m discontinuity in δ^7Li (Fig. 2).

Saprolites from the upper 6 m of the profile have low lithium concentrations and are significantly lighter than the diabase (Fig. 2), features that can be explained by progressive leaching of lithium from the diabase protolith. However, like the saprolites developed on granite, these data do not fall on a single Rayleigh distillation curve, but rather show a range of apparent α values from 0.995 to 0.980 (Fig. 6).

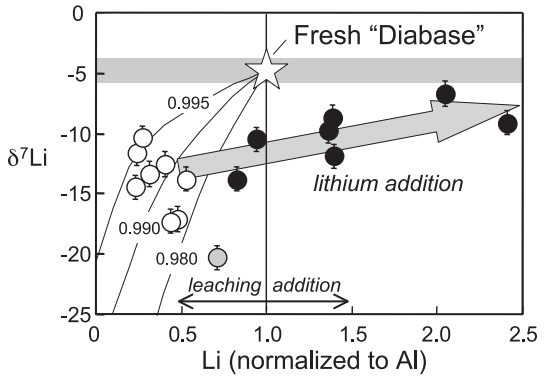

Fig. 6. Normalized lithium concentration vs. δ^7Li for saprolites developed on the Cayce diabase dike. Star shows composition of unweathered diabase. Error bars represent 2σ uncertainty. Curved lines depict lithium removal via Rayleigh distillation for different values (0.995 to 0.980) of the fractionation factor α. Saprolites from upper part of profile (open circles) show correlation between apparent α value and kaolinite/smectite (K/S) ratio: all samples with apparent α less than 0.990 have K/S>2, whereas samples with higher apparent α (0.995 to 0.990) have K/S<0.1. Arrow depicts possible mixing trend in samples lying below the inferred paleo water table (filled symbols) between isotopically light saprolite and heavy lithium from groundwaters. The sample from the 6-m discontinuity lies off all other trends and its extremely light isotopic composition is enigmatic.

Interestingly, saprolites from this upper profile that fall near the Rayleigh distillation curves with lower apparent α values (samples M7 through M10) have higher kaolinite/smectite ratios, which may imply a mineralogical control on isotopic fractionation (e.g., Pistiner and Henderson, 2003), with kaolinite-rich samples exhibiting more fractionation.

There is a rough, negative correlation between lithium content and δ^7Li, with the shallowest samples having the heaviest δ^7Li and the lowest lithium contents. This correlation is difficult to explain. One expects weathering to be most intense at the shallowest levels, where the greatest amount of leaching occurs due to rainwater infiltration. Indeed, the shallowest samples have the lowest density and lowest lithium concentration of the profile, consistent with intense leaching. Yet, these shallow samples do not have the lowest δ^7Li. Indeed, δ^7Li decreases systematically with depth in this upper section of saprolite. Rainwater may have heavy lithium if it contains significant marine aerosols, as seawater is very heavy (~32‰). Addition of marine aerosols was invoked to explain the isotopically heavy lithium seen in the upper portions of Hawaiian soil horizons (Huh et al., 2002; Pistiner and Henderson, 2003) and also in a laterite formed on the Deccan basalts (Kisakurek et al., 2004). However, if the heavier lithium near the surface were due to addition of marine aerosols to the saprolites formed on the diabase dike, lithium concentration should increase, as seen in the Hawaiian soils and the Deccan laterite. The opposite is observed in our study. We thus regard this trend as enigmatic.

The saprolite at 6 m depth (M10), which has the most extreme δ^7Li (−20‰), is only slightly depleted in lithium relative to the fresh diabase and would require extremely low α to explain through Rayleigh distillation (Fig. 6). We thus consider the isotopic composition of this sample to be enigmatic.

Saprolites from below 6 m depth have highly variable lithium contents, with most showing lithium enrichment relative to the unweathered diabase (Fig. 6). These lower samples require addition of heavy lithium to the regolith. We suggest that this was accomplished through sorption of heavy groundwater lithium and thus we suggest that the 6-m depth represents a paleo water table. Although no data exist for groundwater from this region, groundwaters elsewhere are isotopically heavy (+7‰ to +36‰; Hogan and Blum, 2003; Tomascak et al., 2003), which is also consistent with the heavy isotopic composition of river waters, which derive mainly from groundwaters.

6. Conclusions

Results for the lithium isotopic composition of two saprolites developed on igneous rocks in South Carolina (a granite and a diabase dike) demonstrate that the saprolites are consistently isotopically lighter than the unweathered igneous rocks on which they formed, and that δ^7Li correlates negatively with the degree of weathering, as indicated by the chemical index of alteration (CIA) and bulk densities. These results are thus consistent with the widely held view that continental weathering releases heavy lithium to the hydrosphere, leaving isotopically light lithium behind in the regolith.

Development of saprolite on the granite led to a slight decrease in δ^7Li, of up to 2‰ relative to the fresh igneous rock, over a wide range of weathering

intensities, suggesting that lithium leaching was accompanied by only a slight decrease in δ^7Li. The most weathered sample of granite saprolite occurs adjacent to a secondary soil horizon developed on the present hill slope. This sample has a much lighter δ^7Li (−6.8‰), suggesting that a second episode of weathering caused greater isotopic fractionation. The lithium concentration and δ^7Li of the saprolite developed on the granite can be explained by lithium leaching via Rayleigh distillation. However, the data do not lie on a single Rayleigh distillation line, suggesting either that variable fractionation factors applied during weathering or that some of the saprolites also experienced addition of heavy, hydrospheric lithium.

A second profile through saprolite developed on a diabase dike shows extreme isotopic fractionation (δ^7Li from −6.7‰ to −20‰) relative to the unweathered protolith (−4.3‰). The nature of the fractionation in this profile depends on the position of the samples relative to an inferred paleo water table at a depth of 6 m. Above 6 m, the saprolite samples are isotopically light and depleted in lithium, consistent with lithium leaching during progressive weathering. Below 6 m, the δ^7Li varies widely (−14‰ to −6‰), while normalized lithium concentrations are greater than that of the unweathered diabase. These data thus cannot be explained by lithium leaching. A positive correlation between δ^7Li and Li content in these deeper samples suggests they formed as mixtures between an isotopically light saprolite (~−15‰) and heavier lithium derived from groundwater.

Acknowledgements

This work was initiated as the senior thesis of H.B. Njo and was supported by the N.S.F (EAR 0208012). We thank Fang-zhen Teng and Bill McDonough for discussions and L. Chan, T. Moriguti and S.-Y. Jiang for comments that helped us hone our arguments and clarify the manuscript. **[RR]**

References

Bottomley, D.J., Katz, A., Chan, L.H., Starinsky, A., Douglas, M., Clark, I.D., Raven, K.G., 1999. The origin and evolution of Canadian shield brines: evaporation or freezing of seawater? New lithium isotope and geochemical evidence from the Slave craton. Chem. Geol. 155 (3–4), 295–320.

Bottomley, D.J., Chan, L.H., Katz, A., Starinsky, A., Clark, I.D., 2003. Lithium isotope geochemistry and origin of Canadian shield brines. Ground Water 41 (6), 847–856.

Bouman, C., Elliott, T., Uroon, P.Z., 2004. Lithium inputs for subduction zones. Chem. Geol.

Bryant, C.J., Chappell, B.W., Bennett, V., McCulloch, M.T., 2003. Lithium isotopic variations in Eastern Australian granites. Geochim. Comsmochim. Acta 67 (18), A47.

Chan, L.H., Edmond, J.M., 1988. Variation of lithium isotope composition in the marine-environment—a preliminary-report. Geochim. Cosmochim. Acta 52 (6), 1711–1717.

Chan, L.H., Frey, F.A., 2003. Lithium isotope geochemistry of the Hawaiian plume: results from the Hawaii Scientific Drilling Project and Koolau volcano. Geochem. Geophys. Geosyst. 4 doi:10.1029/2002GC000365.

Chan, L.H., Edmond, J.M., Thompson, G., Gillis, K., 1992. Lithium isotopic composition of submarine basalts—implications for the lithium cycle in the oceans. Earth Planet. Sci. Lett. 108 (1–3), 151–160.

Chan, L.H., Alt, J.C., Teagle, D.A.H., 2002. Lithium and lithium isotope profiles through the upper oceanic crust: a study of seawater–basalt exchange at ODP Sites 504B and 896A. Earth Planet. Sci. Lett. 201 (1), 187–201.

Flesch, G.D., Anderson, A.R.J., Svec, H.J., 1973. A secondary isotopic standard for ^{6}Li/^{7}Li determinations. Int. J. Mass Spectrom. Ion Process. 12 (265–272).

Gardner, L.R., Nelson, G.K., 1991. Ghost core stones in granite saprolite near Liberty Hill, South-Carolina. J. Geol. 99 (5), 776–779.

Gardner, L.R., Kheoruenromne, I., Chen, H.S., 1978. Isovolumetric geochemical investigation of a buried granite saprolite near Columbia, SC, USA. Geochim. Cosmochim. Acta 42 (4), 417–424.

Gardner, L.R., Kheoruenromne, I., Chen, H.S., 1981. Geochemistry and mineralogy of an unusual diabase saprolite near Columbia, South-Carolina. Clays Clay Miner. 29 (3), 184–190.

Hogan, J.F., Blum, J.D., 2003. Boron and lithium isotopes as groundwater tracers: a study at the Fresh Kills Landfill, Staten Island, New York, USA. Appl. Geochem. 18 (4), 615–627.

Huh, Y., Chan, L.H., Edmond, J.M., 2001. Lithium isotopes as a probe of weathering processes: Orinoco River. Earth Planet. Sci. Lett. 194 (1–2), 189–199.

Huh, Y., Chan, L.H., Chadwick, O., 2002. Lithium isotopes as a probe of weathering processes: Hawaiian soil climosequence. Geochim. Cosmochim. Acta 66 (15A), A346.

Kisakurek, B., Widdowson, M., James, R.H., 2004. Behaviour of Li isotopes during continental weathering: the Bidar laterite profile, India. Chem. Geol. 72, 27–44 (this volume).

Li, Y.H., 1982. A brief discussion on the mean oceanic residence time of elements. Geochim. Cosmochim. Acta 46 (12), 2671–2675.

McLennan, S.M., 1993. Weathering and global denudation. J. Geol. 101 (2), 295–303.

Moriguti, T., Nakamura, E., 1998. High-yield lithium separation and the precise isotopic analysis for natural rock and aqueous samples. Chem. Geol. 145 (1–2), 91–104.

Nesbitt, H.W., Young, G.M., 1982. Early Proterozoic climates and plate motions inferred from major element chemistry of lutites. Nature 299, 715–717.

Pavich, M.J., Obermeier, S.F., 1985. Saprolite formation beneath coastal-plain sediments near Washington, DC. Geol. Soc. Amer. Bull. 96 (7), 886–900.

Pistiner, J.S., Henderson, G.M., 2003. Lithium-isotope fractionation during continental weathering processes. Earth Planet. Sci. Lett. 214 (1–2), 327–339.

Qi, H.P., Taylor, P.D.P., Berglund, M., De Bievre, P., 1997. Calibrated measurements of the isotopic composition and atomic weight of the natural Li isotopic reference material IRMM-016. Int. J. Mass Spectrom. 171 (1–3), 263–268.

Ryan, J.G., Kyle, P.R., 2000. Lithium isotope systematics of McMurdo volcanic group lavas, and other intraplate suites. Eos Trans. AGU 81 (48) (Fall Meeting Supplement, Abstract V21G-05).

Seitz, H.-M., Brey, G.P., Lahaye, Y., Durali, S., Weyer, S., 2004. Lithium isotopic signatures of peridotite xenoliths and isotopic fractionation at high temperature between olivine and pyroxenes. Chem. Geol.

Teng, F.-z., McDonough, W.F., Rudnick, R.L., Dalpe, C., Tomascak, P.B., Chappell, B.W., Gao, S., 2004. Lithium isotopic composition and concentration of the upper continental crust. Geochim. Cosmochim. Acta (in press).

Tomascak, P.B., Langmuir, C.H., 1999. Lithium isotope variability in MORB. Eos 80, F1086–F1087.

Tomascak, P.B., Carlson, R.W., Shirey, S.B., 1999. Accurate and precise determination of Li isotopic compositions by multi-collector sector ICP-MS. Chem. Geol. 158 (1–2), 145–154.

Tomascak, P.B., Tera, F., Helz, R.T., Walker, R.J., 1999. The absence of lithium isotope fractionation during basalt differentiation: new measurements by multicollector sector ICP-MS. Geochim. Cosmochim. Acta 63 (6), 907–910.

Tomascak, P.B., Hemming, N.G., Hemming, S.R., 2003. The lithium isotopic composition of waters of the Mono Basin, California. Geochim. Cosmochim. Acta 67 (4), 601–611.

White, A.F., 2003. Natural weathering rates of silicate minerals. In: Drever, J.I. (Ed.), Surface and Ground Water, Weathering, and Soils. Treatise on Geochemistry. Elsevier-Pergamon, Oxford, pp. 133–168.

White, A.F., Bullen, T.D., Schulz, M.S., Blum, A.E., Huntington, T.G., Peters, N.E., 2001. Differential rates of feldspar weathering in granitic regoliths. Geochim. Cosmochim. Acta 65 (6), 847–869.

Williams, L.B., Hervig, R.L., 2003. Lithium isotopic fractionation in subduction zones: clues from clays. Eos Trans. AGU 84 (46) (Fall Meeting Supplement, Abstract V52A-0417).

You, C.F., Castillo, P.R., Gieskes, J.M., Chan, L.H., Spivack, A.J., 1996. Trace element behavior in hydrothermal experiments: implications for fluid processes at shallow depths in subduction zones. Earth Planet. Sci. Lett. 140 (1–4), 41–52.